HortScience 52(11):1464–1470. 2017. doi: 10.21273/HORTSCI12259-17

Influence of High Temperature on Photosynthesis, Antioxidative Capacity of Chloroplast, and Carbon Assimilation among Heat-tolerant and Heat-susceptible Genotypes of Nonheading Chinese Cabbage

Lingyun Yuan[1], Yujie Yuan[1], Shan Liu, Jie Wang, Shidong Zhu, Guohu Chen, Jinfeng Hou, and Chenggang Wang[2]

Vegetable Genetics and Breeding Laboratory, School of Horticulture, Anhui Agricultural University, Hefei 230036, China

Additional index words. Brassica campestris, carbohydrate metabolism

***Abstract*. High temperature (HT) is a major environmental stress limiting oversummer production of nonheading Chinese cabbage (NHCC, *Brassica campestris* ssp. *chinensis* Makino). In the present study, the effects of HT on photosynthetic capacity, including light reaction and carbon assimilation, were completely investigated in two NHCC, 'xd' (heat-tolerant), and 'sym' (heat-susceptible). The two genotypes showed significant differences in plant morphology, photosynthetic capacity, and photosynthate metabolism (carboassimilation). HT caused a decrease in photosynthesis, chlorophyll contents, and photochemical activity in NHCC. However, these main photosynthetic-related parameters, including net photosynthetic rate (P_N), maximal photochemical efficiency of PSII (Fv/Fm), and total chlorophyll content in 'xd', were significantly higher than those of 'sym' plants. The antioxidant contents and antioxidative enzyme activities of ascorbic acid-reduced glutathione cycle in the chloroplast of 'xd' were significantly higher than those of 'sym'. Microscopic analyses revealed that HT affected the structure of photosynthetic apparatus and membrane integrity to a different extent, whereas 'xd' could maintain a better integrated chloroplast shape and thylakoid. Inhibited light reaction also hampered carbon assimilation, resulting in a decline of carboxylation efficiency and imbalance of carbohydrate metabolism. However, larger declined extents in these data were presented in 'sym' (heat-susceptible) than 'xd' (heat-tolerant). The heat-tolerant genotype 'xd' had a better capacity for self-protection by improved light reaction and carbon assimilation responding to HT stress.**

Climate model predicts that the average global temperature will increase 1.8 to 4 °C before the end of the 21st century. The additional warming above 2 °C could result in losses of more than 25% to crop yield (IPCC, 2014). Global-scale assessment by IPCC (2013) revealed that the frequency of extreme high temperature (HT) has increased in large parts of Asia, Australia, and Europe. HT could hamper plants growth or cause considerable pre- and postharvest losses because of shortened life cycle and accelerated senescence. The photosynthesis in C_3 plant is more sensitive to HT, especially the photosynthetic apparatus (Wahid and Rasul, 2005). HT differently affects the stability of many proteins and membrane system and alters the efficiency of enzymatic reactions in the cell (Hemantaranjan et al., 2014). Diminished photosynthetic capacity is a primary damage effect by HT. Therefore, research on photosynthetic capacity in vegetable plants has become a crucial approach to evaluate the heat tolerance of vegetable genotypes.

NHCC is one of the most important vegetables in China and is now cultivated around the world. It is very popular in the world and has a great market demand. NHCC is sensitive to heat stress and it could cause inevitable injury. To achieve oversummer production and meet the needs of year-round market, it is important to breed heat-tolerant NHCC genotype by exploring the heat tolerance mechanisms in various genotypes.

The present study was carried out with two genotypes NHCC (heat-tolerant and heat-susceptible) to investigate the photosynthetic capacity, including photosynthesis, antioxidative system, and ultrastructure of chloroplast, and photosynthate metabolism responding to HT. Determination of responses and possible strategies to improve HT tolerance is significant to NHCC to select and breed heat-tolerant genotype.

Materials and Methods

Plants materials and experimental design. Seeds of NHCC cultivars were germinated in pots in a phytotron at Anhui Agricultural University. Germinated seedlings were grown under controlled conditions (day/night 20 °C/15 °C), *PPF* density (PPFD) of 600 $\mu mol \cdot m^{-2} \cdot s^{-1}$, relative humidity of 70%, and a photo period of 14/10 h (light/dark). The seedlings were cultivated under normal growth conditions.

Plants with the six-leaf stage were divided into two groups, respectively. The control group was kept at 20 °C/15 °C. Based on the previous experiment, the treatment groups were subjected to HT at 37 °C/27 °C. The control group of growth condition was similar to the one previously described. After 6 d, the plants were sampled for physiological and biochemical analyses. The seedlings were organized in a complete randomized block design.

Growth parameters. Growth parameters were obtained from 15 seedlings in each replication. Plant height, leaf length, leaf width, petiole length, and petiole width were measured by a ruler. Stem diameter was measured by a vernier caliper. The shoot fresh weight was directly weighted, then the seedlings were dried in an oven at 75 °C for 48 h to gain the shoot dry weight.

Chlorophyll (Chl) contents. The Chl content was determined as the method of Strain and Svec (1966). The pigments were extracted from the forth fully expanded leaf with a mixed solution containing acetone, ethanol, and water (the volume ratio, 4.5:4.5:1).

Photosynthetic parameters and CO_2 exchange. Net photosynthetic rate (P_N), stomatal conductance (g_s), intercellular CO_2 concentration (Ci), and transpiration rate (Tr) were measured using a portable photosynthetic system Li-6400 (LI-COR, Inc., USA) on the forth fully expanded leaf, which is numbered from the center of the plant. Carboxylation efficiency (CE) was calculated using the following relationship: $CE\ (\%) = (P_N/Ci) \times 100$.

Simultaneously, the CO_2 assimilation vs. Ci (A/Ci) curve was measured at a PPFD of 700 $\mu mol \cdot m^{-2} \cdot s^{-1}$ with Li-6400. The maximum carboxylation rate of Rubisco ($V_{c,max}$) and maximum rates of RuBP regeneration (J_{max}) were estimated by fitting a maximum likelihood regression below and above the inflexion of the A/Ci response curve according to McMurtrie and Wang (1993).

Chl fluorescence. The Chl fluorescence was measured using a portable fluorometer (PAM 2100; Walz, Effeltrich, Germany) as per Kooten and Snel (1990). The fully expanded forth leaves were dark-adapted for 30 min before measurement. Fo and Fm are the minimal and maximal fluorescence yield

Received for publication 29 June 2017. Accepted for publication 30 Aug. 2017.

This work was funded by the National Natural Science Foundation of China (No. 31701910), the National Key R & D Program of China (2017YFD0101803), Anhui College Natural Science Project (KJ2017ZD15), and Provincial Natrural Science Foundation of Anhui, China (1608085QC48).

[1]These authors contributed equally to this article.

[2]Corresponding author. E-mail: cgwang@ahau.edu.cn.

of leaves after dark adaptation, respectively; Fo′, Fs, and Fm′ are the minimal, steady-state, and maximal fluorescence level in illuminated leaves, respectively. These fluorescence parameters were used to calculate the following: 1) the actual photochemical efficiency of PSII, ΦPSII = (Fm′ – Fs)/Fm′; 2) the photochemical fluorescence quenching coefficient, qP = (Fm′ – Fs)/(Fm′ – Fo′); 3) nonphotochemical quenching coefficient, qN = (Fm – Fm′)/(Fm′ – Fo′); and 4) the maximal photochemical efficiency of PSII, Fv/Fm = (Fm – Fo)/Fm.

Isolation of chloroplast. Chloroplast isolation was carried out in accordance with the method of Joly and Carpentier (2011) with slight modifications. Forty gram of leaves were grinded in about 150 mL of buffer A (50 mM Hepes NaOH, 330 mM sorbitol, 2 mM EDTA, 1 mM $MgCl_2$ and 1 mM $MnCl_2$), and the homogenate was filtered two times on two layers of Miracloth tissue. The filtrate was centrifuged at 750 × *g* for 60 s. The supernatant was discarded, and the pellet was resuspended in about 30 mL of buffer B (50 mM Hepes-NaOH, 330 mM sorbitol, 2 mM EDTA, 1 mM $MgCl_2$, 1 mM $MnCl_2$, 10 mM KCl and 1 mM NaCl). Then, the mixture was centrifuged again, and the supernatant was discarded. Finally, the pellet was resuspended in a small volume of buffer B (1.5 mL). All procedures were carried out at 4 °C.

Malondialdehyde (MDA) and hydrogen peroxide (H_2O_2) content in chloroplast. The level of lipid peroxidation was measured by estimating MDA content (a product of lipid peroxidation) using thiobarbituric acid (TBA) according to Xu et al. (2008).

The isolated chloroplast suspension was reacted with a mixture of $TiCl_4$ in 20% H_2SO_4 (v/v) and was measured spectrophotometrically at 415 nm to estimate the H_2O_2 content (Patterson et al., 1984).

Antioxidant content in chloroplast. Ascorbic acid (AsA) and dehydroascorbate (DHA) content were assayed according to Shu et al. (2013). Reduced glutathione (GSH) and oxidized glutathione (GSSG) content were determined by following Griffiths (1980).

Activities of antioxidative enzymes in chloroplasts. Ascorbate peroxidase (APX) activity was measured by Nakano and Asada (1981) with slight modifications. Reaction buffer solution contained 50 mM K-P buffer (pH 7.0), 0.5 mM AsA, 0.1 mM H_2O_2, 0.1 mM EDTA, and chloroplast suspension (0.1 mg/mL Chl). A reaction was started by adding H_2O_2. The APX activity was measured at 290 nm for 1 min using 2.8 $mM^{-1}·cm^{-1}$ of extinction coefficient.

Glutathione reductase (GR) activity was determined by following the method of Hasanuzzaman et al. (2012) with slight modifications. Reaction mixture contained 50 mM K-P buffer (pH 7.8), 0.2 mM EDTA, 10 mM GSSG, 2.4 mM nicotinamide adenine dinucleotide phosphate (NADPH), and chloroplast suspension (0.1 mg/mL Chl). Reaction was initiated with GSSG, and the decrease value in absorbance at 340 nm was recorded for 1 min (calculated using 6.2 $mM^{-1}·cm^{-1}$ of extinction coefficient).

Monodehydroascorbate reductase (MDAR) activity was determined in accordance with the method of Hossain et al. (1984) with slight modifications. Reaction mixture contained 50 mM Hepes-KOH buffer (pH 7.6), 1 mM NADPH, 5 mM AsA, and 0.14 unit of ascorbate oxidase and chloroplast suspension (0.1 mg/mL Chl). A reaction was started by adding ascorbate oxidase. The absorbance was taken at 340 nm. Enzyme activity was calculated from change in absorbance for 1 min using 6.2 $mM^{-1}·cm^{-1}$ of extinction coefficient.

Dehydroascorbate reductase (DHAR) activity was determined in accordance with the method of Nakano and Asada (1981) with slight modifications. Reaction buffer contained 50 mM K-P buffer (pH 7.0), 50 mM GSH, and 10 mM DHA. The activity was calculated from change in absorbance at 265 nm for 1 min using 14 $mM^{-1}·cm^{-1}$ of extinction coefficient.

Chloroplast ultrastructure. The ultrastructure of chloroplast was analyzed by electron microscopy. Fully expanded forth leaves were cut into pieces (≤0.1 × 0.5 cm) and immediately immersed in 2.5% glutaraldehyde in 0.1 M phosphate buffer for 24 h incubation at 4 °C (primary fixation). The pieces were then immersed in 1% (w/v) osmium tetroxide to increase fixation and washed several times with 0.1 M phosphate buffer. The fixed samples were dehydrated through successive acetone washes and finally embedded in Spurr's epoxy resin. Ultrathin sections were cut on an ultramicrotome, stained with 2.5% (w/v) uranyl acetate followed by lead citrate. Embedded sections were observed under a transmission electron microscope (H-7650; Hitachi, Tokyo, Japan) at an accelerating voltage of 80 kV.

Carbohydrate content and carbohydrate-related enzyme activities. Total soluble sugar, sucrose, fructose, and starch content were determined according to Buysse and Merckx (1993) using a modified phenol–sulphuric acid method. The freeze-dried samples were sampled for the determination of carbohydrate content.

Sucrose phosphate synthase (SPS) (EC 2.4.1.14) and sucrose synthase (SS) (EC 2.4.1.13) were extracted at 0 ± 4 °C according to Lowell et al. (1989). SPS activity was assayed at 37 °C by the method of Hubbard et al. (1989). SS activity for sucrose cleavage was assayed in accordance with the method of Lowell et al. (1989). Acid invertase (AI) (EC 3.2.1.26) was extracted following the method described by Miron and Schaffer (1991). Amylase (EC 3.2.1.1) was measured as described by Miyagi et al. (1990) and Doehlert et al. (1982).

Statistical analyses. The data were statistical analyzed with SAS software (SAS Institute, Cary, NC) and Duncan's multiple range test at the $P < 0.05$ level of significance.

Results

Morphology parameters. Compared with control, stem diameter, fresh, and dry weights of shoot in heat-susceptible genotype 'sym' (HT-sym) were significantly decreased by 32.08%, 19.19%, and 23.08%, respectively, whereas an increase in plant height was by 19.85% (Table 1). In heat-tolerant genotype 'xd' (HT-xd), the stem diameter, fresh, and dry weights of shoot were also decreased by 19.47%, 18.90%, and 12.77%, respectively, and the plant height was unaffected under HT. The stem diameter and shoot dry weight of 'xd' were more than that of 'sym' exposed to HT.

Compared with control, the petiole length and width of HT-sym treatment were obviously decreased by 10.19% and 21.92%, respectively, whereas the leaf length was increased by 18.89%. HT caused a decrease in the leaf length of 'xd', whereas the other indexes of leaf morphology had no obvious changes. Under HT, the leaf width and petiole length of 'sym' were more than that of 'xd', and the petiole width of 'sym' was lower than 'xd'.

Under control condition, the plant height, leaf length, leaf width, and petiole length in 'sym' were more than that of 'xd', and the stem diameter, shoot biomass, and petiole width of 'sym' were lower than that of 'xd'.

Chl content. Compared with respective control, Chl a, b, and a + b content of HT-sym were significantly decreased by 18.27%, 24.41%, and 20.31% and those of HT-xd were 9.03%, 7.52%, and 14.69%, respectively (Table 2). Under normal condition, Chl a and a + b content of 'xd' were obviously higher than that of 'sym'.

Photosynthetic parameters. Under HT, P_N, g_s, Ci, Tr, and CE of two genotypes

Table 1. Effects of high temperature on plant morphology in two nonheading Chinese cabbage cultivars.

Treatment	Plant ht (cm)	Stem diam (mm)	Shoot fresh wt (g)	Shoot dry wt (g)
Cont-sym	9.07 ± 0.93 b	3.99 ± 0.20 b	5.16 ± 0.37 b	0.39 ± 0.03 b
Cont-xd	9.33 ± 0.61 b	4.52 ± 0.21 a	5.66 ± 0.27 a	0.47 ± 0.02 a
HT-sym	10.87 ± 0.21 a	2.71 ± 0.18 d	4.17 ± 0.20 d	0.30 ± 0.03 c
HT-xd	8.97 ± 0.93 b	3.64 ± 0.05 c	4.89 ± 0.12 c	0.41 ± 0.04 b
Treatment	Leaf length (cm)	Leaf width (cm)	Petiole length (cm)	Petiole width (mm)
Cont-sym	5.77 ± 0.31 c	4.87 ± 0.14 b	8.83 ± 0.21 a	0.73 ± 0.03 b
Cont-xd	6.43 ± 0.2 b	5.83 ± 0.32 a	6.03 ± 0.26 c	0.87 ± 0.04 a
HT-sym	6.86 ± 0.17 a	4.67 ± 0.32 b	7.93 ± 0.32 b	0.57 ± 0.02 c
HT-xd	5.91 ± 0.18 c	5.40 ± 0.27 a	6.07 ± 0.40 c	0.83 ± 0.05 ab

Values are represented as the mean ± SE (n = 15). Different letters in the same column indicate significant differences at $P < 0.05$ according to Duncan's multiple range tests.

NHCC showed similar declined trends (Fig. 1). Compared with respective control, P_N of HT-sym and HT-xd were decreased by 61.95% and 37.68%; g_s of HT-sym and HT-xd were 57.38% and 34.65%; Tr were 65.91% and 33.33%; Ci were 62.75% and 33.59%, and CE were 59.96% and 26.74%. From the Fig. 1, the declined range of HT-sym was more than HT-xd. Under control, P_N and Tr of Cont-xd were higher than Cont-sym.

$V_{c,max}$ and J_{max}. $V_{c,max}$ and J_{max} of two genotypes were significantly reduced by HT (Fig. 6). The $V_{c,max}$ of HT-sym and HT-xd were decreased by 36.44% and 23.59%, respectively, whereas the J_{max} of two genotypes were 22.74% and 20.55%. J_{max} of Cont-xd was higher than Cont-sym, and $V_{c,max}$ of two genotypes had no change under control.

Fluorescence parameters. The ΦPSII, qP and Fv/Fm of HT-sym, and HT-xd were significantly decreased compared with their respective control (Fig. 2). Compared with control, ΦPSII of HT-sym and HT-xd were decreased by 39.35% and 30.15% (Fig. 2A); qP of HT-sym and HT-xd were 32.43% and 27.36% (Fig. 2B); Fv/Fm were 10.48% and 3.14% (Fig. 2D). Aforementioned data showed that the declined degree of ΦPSII, qP, and Fv/Fm in HT-sym was more than HT-xd. The qN of HT-xd reached the highest value among all treatments, which was increased by 33.93% than HT-sym (Fig. 2C).

Under normal condition, ΦPSII and qP of Cont-xd were higher than that of Cont-sym, whereas qN and Fv/Fm of two genotypes had no difference.

MDA and H_2O_2 content in chloroplast. After 6 d of HT treatment, the MDA content of HT-sym and HT-xd were significantly increased by 54.59% and 29.28%, respectively, to the control (Fig. 3A). The H_2O_2 content of HT-sym showed a 1.98-fold increase to Cont-xym, and HT-xd was 1.48-fold to Cont-xd (Fig. 3B). Under normal condition, the MDA and H_2O_2 contents of two genotypes were similar.

Antioxidant content in chloroplasts. Under HT, the total AsA content of HT-sym and HT-xd were significantly declined by 15.63% and 12.16%, respectively, compared with the control (Table 3). The AsA levels of HT-sym and HT-xd were remarkably decreased by 46.04% and 25.71%, respectively. DHA level of HT-sym was higher than other treatments. Compared with control, the AsA/DHA ratios of HT-sym and HT-xd were declined by 58.22% and 32.93%, respectively. Under normal condition, levels of the total AsA, AsA, DHA, and AsA/DHA ratio had no significant difference between Cont-sym and Cont-xd.

Compared with control, the total glutathione levels of HT-sym and HT-xd were markedly increased by 12.84% and 36.21%, respectively (Table 4). The GSH of HT-sym was decreased by 40.33% to the control, whereas that of HT-xd reached a 1.40-fold increase in the control. Among all treatments, the HT-sym had the highest level of GSSG. The GSH/GSSG ratio of HT-sym was the lowest among treatments, whereas that of HT-xd got the highest value. Under normal condition, levels of the total glutathione, GSH, GSSG, and GSH/GSSG ratio were similar between Cont-sym and Cont-xd.

Activities of antioxidative enzymes in chloroplast. HT obviously enhanced the activities of APX by 30.44% and 33.39%, respectively, in HT-sym and HT-xd (Fig. 4A). The activity of GR showed similar changes as APX; GR activities of HT-sym and HT-xd

Table 2. Effects of high temperature on chlorophyll contents in two nonheading Chinese cabbage cultivars.

	Chl a	Chl b	Chl a + b
Cont-sym	8.35 ± 0.10 b	4.14 ± 0.06 a	12.49 ± 0.16 b
Cont-xd	9.25 ± 0.21 a	4.11 ± 0.09 a	13.36 ± 0.26 a
HT-sym	6.83 ± 0.18 d	3.13 ± 0.05 c	9.95 ± 0.16 d
HT-xd	7.60 ± 0.16 c	3.80 ± 0.10 b	11.40 ± 0.26 c

Values are represented as the mean ± SE (n = 3). Different letters in the same column indicate significant differences at $P < 0.05$ according to Duncan's multiple range tests.

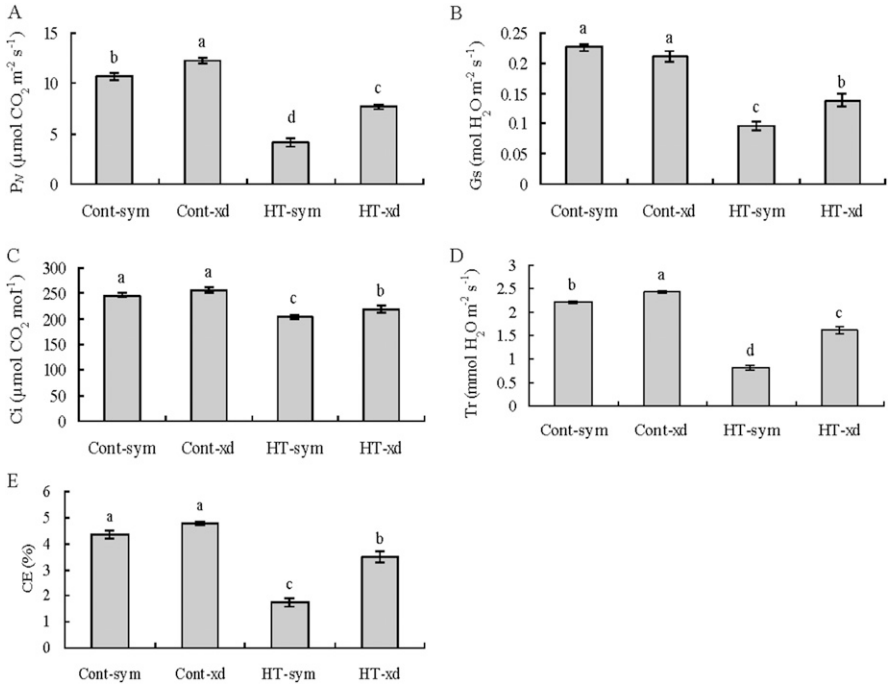

Fig. 1. Effects of high temperature on photosynthesis in two NHCC genotypes. Values represent the mean ± SE (n = 3). Different letters in the same column indicate significant differences at $P < 0.05$ according to Duncan's multiple range tests.

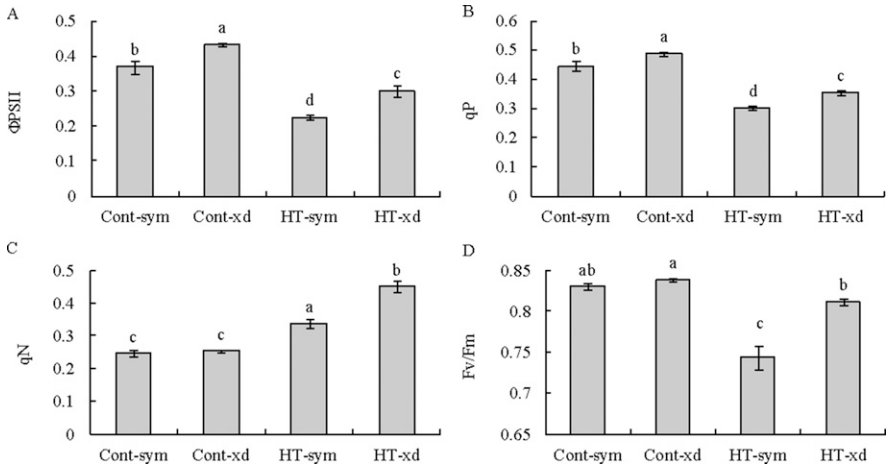

Fig. 2. Effects of high temperature on chlorophyll fluorescence parameters in two NHCC genotypes. Values represent the mean ± SE (n = 3). Different letters in the same column indicate significant differences at $P < 0.05$ according to Duncan's multiple range tests.

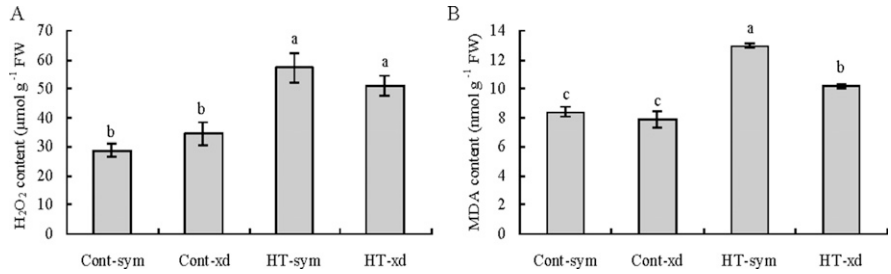

Fig. 3. Effects of high temperature on H_2O_2 content and Malondialdehyde content in two NHCC genotypes. Values represent the mean ± SE (n = 3). Different letters in the same column indicate significant differences at $P < 0.05$ according to Duncan's multiple range tests.

Table 3. Effects of high temperature on total AsA, AsA, DHA, and AsA/DHA in two nonheading Chinese cabbage cultivars.

	AsA + DHA	AsA	DHA	AsA/DHA
Cont-sym	8.96 ± 0.06 ab	5.30 ± 0.20 a	3.66 ± 0.15 b	1.46 ± 0.12 ab
Cont-xd	9.54 ± 0.30 a	5.95 ± 0.32 a	3.59 ± 0.22 b	1.67 ± 0.17 a
HT-sym	7.56 ± 0.40 c	2.86 ± 0.18 c	4.70 ± 0.25 a	0.61 ± 0.03 c
HT-xd	8.38 ± 0.24 bc	4.42 ± 0.27 b	3.96 ± 0.14 b	1.12 ± 0.09 b

AsA = ascorbic acid; DHA = dehydroascorbate.
Values are represented as the mean ± SE (n = 3). Different letters in the same column indicate significant differences at $P < 0.05$ according to Duncan's multiple range tests.

Table 4. Effects of high temperature on total GSH, GSH, GSSG, and GSH/GSSG in two nonheading Chinese cabbage cultivars.

	GSH + GSSG	GSH	GSSG	GSH/GSSG
Cont-sym	17.14 ± 0.54 c	14.01 ± 0.58 b	3.13 ± 0.03 b	4.48 ± 0.23 b
Cont-xd	17.87 ± 0.19 bc	14.86 ± 0.20 b	3.01 ± 0.15 b	4.96 ± 0.30 b
HT-sym	19.34 ± 0.28 b	8.36 ± 0.51 c	10.98 ± 0.31 a	0.77 ± 0.07 c
HT-xd	24.34 ± 0.82 a	20.77 ± 0.81 a	3.58 ± 0.07 b	5.81 ± 0.25 a

GSH = reduced glutathione; GSSG = oxidized glutathione.
Values are represented as the mean ± SE (n = 3). Different letters in the same column indicate significant differences at $P < 0.05$ according to Duncan's multiple range tests.

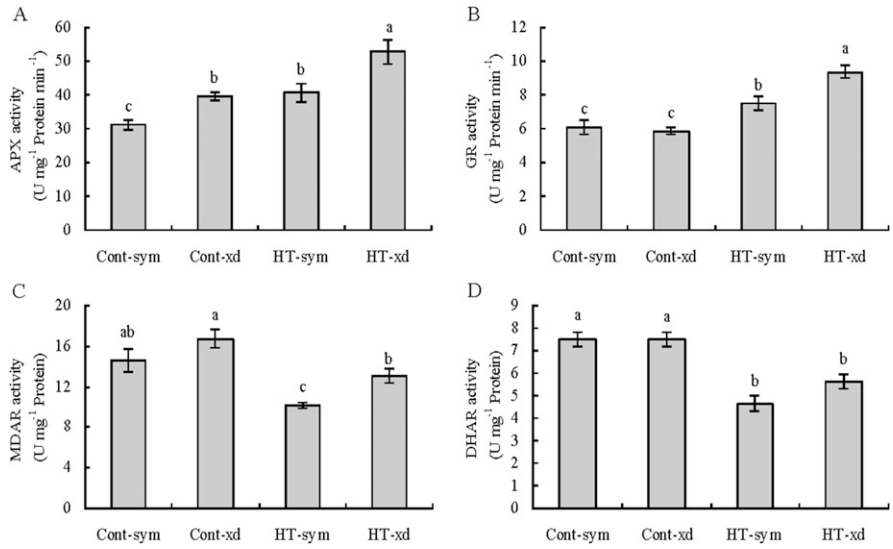

Fig. 4. Effects of high temperature on ascorbate peroxidase (APX), glutathione reductase (GR), monodehydroascorbate reductase (MDAR), and dehydroascorbate reductase (DHAR) activities in two NHCC genotypes. Values represent the mean ± SE (n = 3). Different letters in the same column indicate significant differences at $P < 0.05$ according to Duncan's multiple range tests.

were increased by 23.15% and 59.64%, respectively (Fig. 4B). Compared with the control, significant decreases in the activities of MDAR and DHAR were observed after treatment of HT (Fig. 4C and D). MDAR activities were reduced by 30.37% and 21.68% in HT-sym and HT-xd, respectively. DHAR activity of HT-sym had a reduction by 38.08%, and HT-xd was 24.84%.

Under normal condition, the APX activity of Cont-xd was higher than that of Cont-sym; the activities of GR, MDAR, and DHAR had no significant difference between the two genotypes of NHCC.

Ultrastructure of photosynthetic apparatus. According to the transmission electron micrographs, the chloroplasts of Cont-sym and Cont-xd (Fig. 5A and C) showed a typical oval shape; the grana lamellae (GL) of two genotypes were orderly stacked (Fig. 5B and D). Under HT, the shape of chloroplast was varied from an oval to nearly round in sym, whereas it had no remarkable change in xd. Compared with HT-sym (Fig. 5G), the double membrane system (DMS) of sym chloroplast envelopes was damaged to degradation and became notably disorganized; the SL and GL were induced by HT to partly loosen and disarranged with numerous osmiophilic plastoglobuli. The HT-xd was maintained a better integrated shape of chloroplast and thylakoid with less osmiophilic plastoglobuli accumulation.

Carbohydrate content. The total soluble sugar of HT-sym and HT-xd were higher than their respective control when exposed to HT, which was increased to 2.20- and 2.22-fold, respectively (Table 5). The sucrose content of HT-sym and HT-xd was significantly reduced by 42.51% and 26.16%, respectively, to the control. Fructose content of HT-sym and HT-xd was also declined to the control, which was decreased by 25.76% and 13.37%, respectively. HT caused enhancement of starch in HT-sym and HT-xd by 22.69% and 81.26% to the control. In addition, content of sucrose, fructose, and starch in HT-xd were higher than that of HT-sym.

The content of soluble sugar, sucrose, fructose, and starch had no significant difference between Cont-sym and Cont-xd treatments under normal condition.

Carbohydrate-related enzyme activities. SPS activity of HT-sym was remarkedly declined by 16.13% exposed to HT, whereas that of HT-xd was increased to 1.98-fold to the control (Fig. 7A). Compared with control, the SS activities of HT-sym and HT-xd were markedly decreased by 74.78% and 48.02%, respectively (Fig. 7B). The AI activity of HT-sym was reduced by 38.86% and that of HT-xd was unaffected by HT (Fig. 7C). Amylase activities of HT-sym and HT-xd were declined by 22.72% and 17.20%, respectively, to the control, whereas that of HT-xd was significantly higher than HT-sym (Fig. 7D).

Under normal condition, only SS activity of Cont-xd was higher than Cont-sym, and the rest of the enzyme activities were similar between the two genotypes.

Discussion

HT during development period is a major limiting factor on the economic yield of crop plants, especially leafy vegetable. Therefore, understanding the effects of HT on phenology and the physiological traits linked to tolerance is imperative. In the present study,

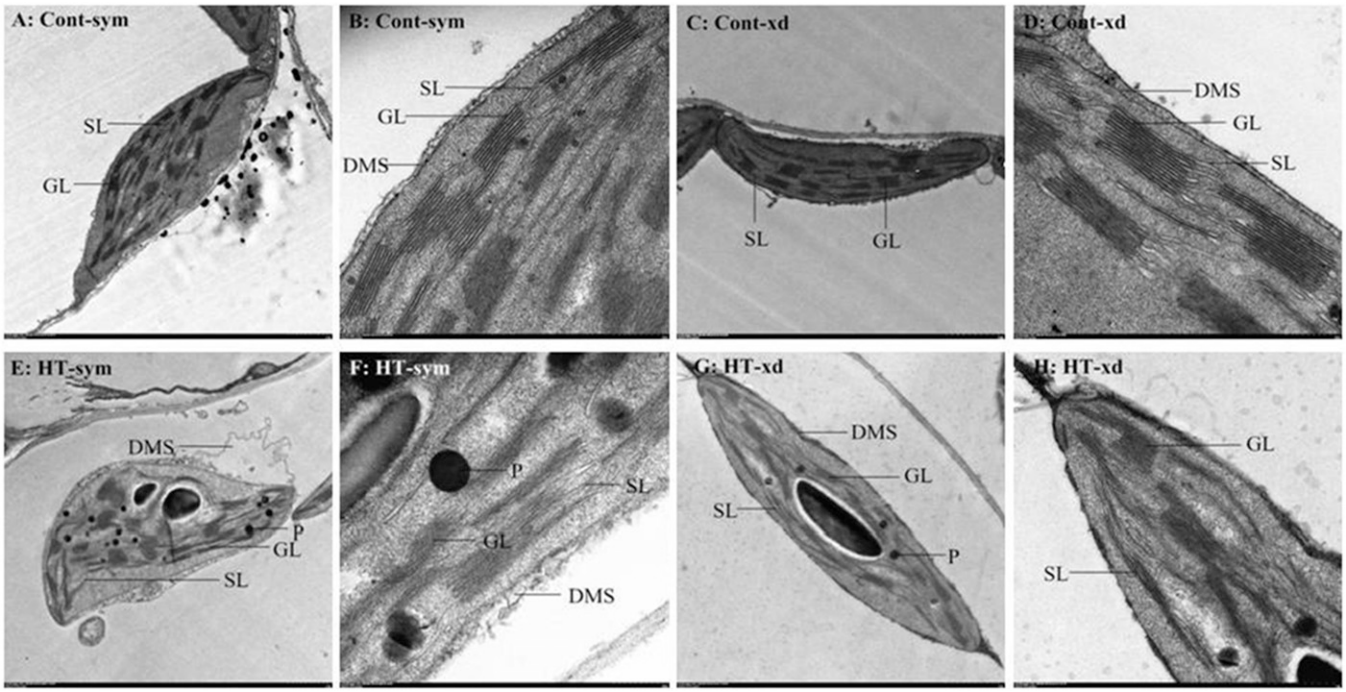

Fig. 5. Transmission electron micrographs showing changes in ultrastructure of chloroplast and thylakoid of two NHCC genotypes under heat stress. Scale bars for chloroplasts and thylakoids are 1 and 0.2 µm, respectively. GL = grana lamellae; SL = stroma lamellae; DMS = double membrane system; P = plastoglobulus.

Table 5. Effects of high temperature on sugar contents in two nonheading Chinese cabbage cultivars.

	Soluble sugar	Sucrose	Fructose	Starch
Cont-sym	37.43 ± 1.17 c	12.72 ± 0.62 d	12.56 ± 1.58 c	0.22 ± 0.01 c
Cont-xd	35.13 ± 2.34 c	15.84 ± 0.81 c	15.31 ± 1.50 c	0.24 ± 0.01 c
HT-sym	51.82 ± 3.09 b	19.03 ± 0.98 b	21.21 ± 0.71 b	0.32 ± 0.01 b
HT-xd	61.74 ± 1.75 a	25.45 ± 0.96 a	27.12 ± 0.88 a	0.39 ± 0.02 a

Values are represented as the mean ± SE (n = 3). Different letters in the same column indicate significant differences at $P < 0.05$ according to Duncan's multiple range tests.

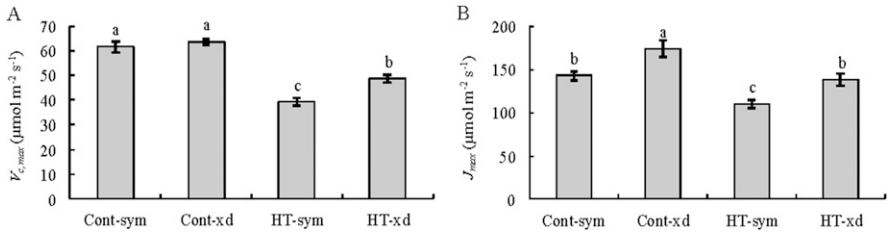

Fig. 6. Effects of high temperature on $V_{c,max}$ and J_{max} in two NHCC genotypes. Values represent the mean ±SE (n = 3). Different letters in the same column indicate significant differences at $P < 0.05$ according to Duncan's multiple range tests.

two genotypes of NHCC showed different responses to heat stress on plant morphology and photosynthetic capacity. The results indicated that heat tolerance of NHCC was genotype specific, consistent with the report of Mishra et al. (2017).

HT treatment caused an increase in the plant height, leaf, and petiole length in heat-susceptible genotype 'sym' than in that of heat-tolerant 'xd' (Table 1). Although HT markedly inhibited biomass accumulation of both genotypes, the decline degrees of shoot fresh and dry weights in heat-tolerant HT-xd were obviously less than heat-susceptible HT-sym. This result presented that NHCC might improve the heat tolerance by regulating plant architecture and leaf shape.

Photosynthesis is one of the most sensitive physiological processes, which is remarkably influenced by HT in C_3 plants (Yang et al., 2006). A great reduction of P_N was linked to the decreases in chlorophyll contents (Table 2) as a result of reduced antenna pigments, restraining the light harvest during HT (Camejo et al., 2006). The alterations by HT in Chl content might be due to impaired biosynthesis or accelerated pigment degradation. Although HT reduced the Chl content, the reduction extent depended on heat tolerance of NHCC against HT. Chl content of heat-susceptible 'sym' was significantly less than heat-tolerant 'xd' (Table 2). Similar to our previous report (Zou et al., 2017) in wucai (*Brassica campestris* L., one of NHCC), an accumulation of Chl might be proposed as one of the potential biochemical indicators of HT tolerant in NHCC. In addition, the result of the present study showed that the rest of the photosynthetic parameters, such as g_s, Ci, and Tr in two genotypes, were also markedly inhibited compared with the control (Fig. 1). The regulation of g_s is a key factor for both desiccation prevention and CO_2 acquisition (showed by Ci). In our study, companied with reduced g_s, Ci also presented the similar reduced trend exposed to HT in two genotypes, which indicated the efficiency reduction of mesophyll cells to use the available CO_2 (Karaba et al., 2007), revealing that the decrease in P_N was attributed to the stomata limitation in the early stage. In our study, accelerating Tr to cool leaf surface temperature was also contributed to the improvement of heat tolerant against HT (Sharma et al., 2014). The declined degree of each index in photosynthesis was lower in heat-tolerant genotype 'xd' than heat-sensitive 'sym', showing a higher gas exchange potential of 'xd' against HT stress.

To further estimate leaf photosynthesis, *A*/Ci curve analysis was used to assess CE, which was mainly associated with the amount, activity, kinetics of Rubisco (explained by $V_{c,max}$), and the rate of ribulose-1, 5-bisphosphate regeneration supported by electron transport (explained by J_{max}); the CE was limited by $V_{c,max}$ more than by J_{max} (Manter and Kerrigan, 2004). The lower $V_{c,max}$ in NHCC exposed to HT (Fig. 6A) might result from lower g_s values

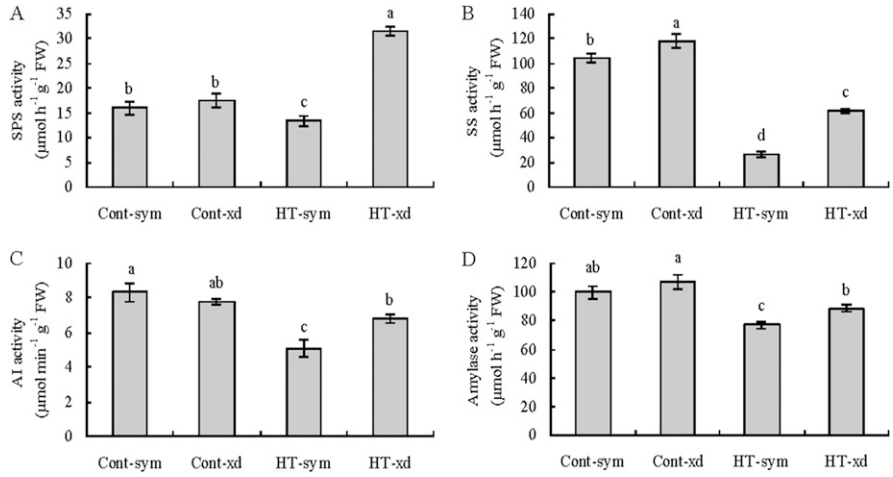

Fig. 7. Effects of high temperature on sucrose phosphate synthase (SPS), sucrose synthase (SS), acid invertase (AI), and Amylase activities in two NHCC genotypes. Values represent the mean ± SE ($n = 3$). Different letters in the same column indicate significant differences at $P < 0.05$ according to Duncan's multiple range tests.

(Fig. 1B), which caused less available CO_2 level (Crafts-Brandner and Law, 2000). Higher $V_{c,max}$ and J_{max} of 'xd', combined with higher CE, indicated more enhancement of CO_2 assimilation than 'sym'. In addition, soluble sugars were accumulated in both heat-susceptible and heat-tolerant genotypes by behaving in osmotic adjustment or acting as nutrient and metabolic signal molecules against osmotic damage (Baena-González et al., 2007). Sucrose is the photosynthetic end-products of CO_2 assimilation. During the sucrose metabolism process, SPS catalyzes the sucrose biosynthesis, and SS and AI are involved in sucrose cleavage in photosynthetic cell as the key enzymes. Sucrose accumulation in heat-susceptible 'sym' was attributed to decreased activities of SS (Fig. 7B) and AI (Fig. 7C), whereas the accumulation in heat-tolerant 'xd' was due to increased SPS enzyme activity exposed to HT stress (Fig. 7A). On the other hand, the accumulation of sucrose in two genotypes might present the carbohydrate translocation and partitioning to sink was largely inhibited by stress (Zhou et al., 2015). Amylase could break down complex sugars, such as starch, into simple sugars. In the present study, higher amylase activity (Fig. 7D), together with higher starch content (Table 5), was induced by HT in heat-tolerant genotype 'xd', showing a stronger capacity of starch biosynthesis and higher substrate availability which was favorable to photosynthesis (Yuan et al., 2014).

Photosynthesis decline was induced and coupled with degradation in the energy conversion efficiency in PSII under HT. PSII is highly sensitive to HT, and its activity is significantly impaired or even partially stopped. Under HT stress, ΦPSII, Fv/Fm, and qP were significantly lessened in heat-tolerant and heat-susceptible genotypes (Fig. 2), indicating that HT led to a clear damage to the PSII, which was consistent with the report of Zha et al. (2016). qN of NHCC was enhanced by HT, which was contrary to the report in tomato (Gerganova et al., 2016). This difference might be due to the cultivar tolerance. Increased qN suggested that thermal dissipation was enhanced, which was induced as the photoprotective mechanism responding to HT (Fig. 2C). The varied extents in chlorophyll fluorescence parameters of heat-tolerant 'xd' were smaller than heat-susceptible 'sym', which revealed that the heat-tolerant genotype had better photochemical activity under HT. Meanwhile, the malfunction of PSII reduced the electron transport efficiency, resulting in further reduced P_N and substantive accumulation of excess electron (causing oxidative stress) under HT stress.

To compare the oxidative damage of photosynthetic apparatus, we investigated the antioxidative system in chloroplast. Severe oxidation damage was found in spinach leaf chloroplast by increased O_2^- and H_2O_2 content under abiotic stress (Zheng et al., 2008). The accumulation of ROS in chloroplast during photosynthesis could cause peroxidation of membrane lipids, destruction of pigments, and modification of membrane function (Xu et al., 2006). According to the microscopic observation of heat-susceptible 'sym', HT caused degradation of thylakoid lamellae and double membrane structure and accumulation of plastoglobuli (Fig. 7), resulting in membrane peroxidation (higher content of MDA and H_2O_2) (Fig. 3). The antioxidant enzyme activities were decreased along with increased ROS accumulation as compared with control, corresponding to the report of Xie et al. (2008). Ascorbate and glutathione protect plants against oxidative stress as the antioxidants. It was reported that the tolerance of wheat varieties appeared to be correlated with the antioxidant level (Balla et al., 2015). In the present study, the reduced AsA and glutathione content of chloroplast in heat-tolerant 'xd' were significantly higher than those of heat-susceptible 'sym' (Tables 3 and 4), which were related with higher antioxidative enzyme activities, including APX, GR, and MDAR (Fig. 4). The higher antioxidative capacity in the chloroplast of 'xd' partly protected the membrane system of thylakoid from oxidative damage (declined MDA and H_2O_2 content).

The chloroplast is the key site for photosynthesis, in which both photochemical reactions and carbon metabolism take place. However, thylakoid membrane is highly sensitive to HT (Wang et al., 2009). In heat-susceptible 'sym', HT altered the structural organization of thylakoids, disrupted the GL stacking, and destroyed the double membrane structure of chloroplast, resulting in the accumulation of plastoglobulus number (Fig. 7). These alterations of chloroplast ultrastructure can negatively and directly influence the photosynthetic apparatus function and inhibit the activities of membrane-associated electron carries and enzymes, which ultimately result in a reduced rate of photosynthesis (Zhang et al., 2014). The swollen chloroplasts and disordered lamellase were more severe in heat-susceptible 'sym', indicating that the chloroplast and thylakoid suffered from more damage than the chloroplast in heat-tolerant 'xd'.

Conclusions

HT considerably hampered the photosynthetic process in NHCC by altering the chlorophyll pigments content, chloroplast ultrastructure, antioxidative capacity of chloroplast, and carbohydrate metabolism homeostasis, resulting in plant growth inhibition. It was demonstrated that heat tolerance of NHCC was associated with the ability to maintain higher photosynthetic capacity in both light and dark reactions, improving the energy conversion and photosynthetic product formations to resistant heat stress damage.

Literature Cited

Baena-González, E., F. Rolland, J.M. Thevelein, and J. Sheen. 2007. A central integrator of transcription networks in plant stress and energy signaling. Nature 448:938–942.

Balla, K., S. Bencze, T. Janda, and O. Veisz. 2015. Analysis of heat stress tolerance in winter wheat. Acta Agron. Hung. 57:437–444.

Buysse, J. and R. Merckx. 1993. An important colorimetric method to quantify sugar content of plant tissue. J. Expt. Bot. 44:1627–1629.

Camejo, D., A. Jiménez, J.J. Alarcón, W. Torres, J.M. Gómez, and F. Sevilla. 2006. Changes in photosynthetic parameters and antioxidant activities following heat-shock treatment in tomato plants. Funct. Plant Biol. 33:177–187.

Crafts-Brandner, S.J. and R.D. Law. 2000. Effect of heat stress on the inhibition and recovery of the ribulose-1, 5-bis-phoshate carboxylase/oxygenase activation state. Planta 212:67–74.

Doehlert, D.C., S.H. Duke, and L. Anderson. 1982. Beta-amylases from alfalfa (*Medicago sativa* L.) roots. Plant Physiol. 69:1096–1102.

Gerganova, M., A.V. Popova, D. Stanoeva, and M. Velitchkova. 2016. Tomato plants acclimate better to elevated temperature and high light than to treatment with each factor separately. Plant Physiol. Biochem. 104:234–241.

Griffiths, O.W. 1980. Determination of glutathione and glutathione disulphide using glutathione reductase and 2-vinylpyridine. Anal. Biochem. 106:207–212.

Hasanuzzaman, M., M.A. Hossain, and M. Fujita. 2012. Exogenous selenium pretreatment protects rapeseed seedlings from cadmium-induced oxidative stress by upregulating antioxidant defence and methylglyoxal detoxification systems. Biol. Trace Elem. Res. 149:248–261.

Hemantaranjan, A., A.N. Bhanu, M.N. Singh, D.K. Yadav, P.K. Patel, R. Singh, and D. Katiyar. 2014. Heat stress responses and thermotolerance. Adv. Plants Agr. Res. 1:1–12.

Hossain, M.A., Y. Nakano, and K. Asada. 1984. Monodehydroascorbate reductase in spinach chloroplasts and its participation in the regeneration of ascorbate for scavenging hydrogen peroxide. Plant Cell Physiol. 25:385–395.

Hubbard, N.L., S.C. Huber, and D.M. Pharr. 1989. Sucrose phosphate synthase and acid invertase as determinants of sucrose accumulation in developing muskmelon (*Cucumis melo* L.) fruits. Plant Physiol. 91:1527–1534.

IPCC. 2013. Climate change 2013: The physical science basis. Contribution of Working Group I to the Fifth Assessment Report of the Intergovernmental Panel on Climate Change. Cambridge University Press, Cambridge, UK.

IPCC. 2014. Climate change 2014: Impacts, adaptation and vulnerability. Summary for policy makers. WG II AR5:13–18.

Joly, D. and R. Carpentier. 2011. Rapid isolation of intact chloroplasts from spinach leaves. Methods Mol. Biol. 684:321–325.

Karaba, A., S. Dixit, R. Greco, A. Aharoni, K.R. Trijatmiko, N. Marsch-Martinez, A. Krishnan, K.N. Nataraja, M. Udayakumar, and A. Pereira. 2007. Improvement of water use efficiency in rice by expression of HARDY, an Arabidopsis drought and salt tolerance gene. Proc. Natl. Acad. Sci. USA 104:15270–15275.

Kooten, O. and J. Snel. 1990. The use of chlorophyll fluorescence nomenclature in plant stress physiology. Photosynth. Res. 25:147–150.

Lowell, C.A., P.T. Tomlinson, and K.E. Koch. 1989. Sucrose-metabolising enzymes in transport tissue and adjacent sink structures in developing citrus fruit. Plant Physiol. 90:1394–1402.

Manter, D.K. and J. Kerrigan. 2004. A/Ci curve analysis across a range of woody plant species: Influence of regression analysis parameters and mesophyll conductance. J. Expt. Bot. 55:2581–2588.

McMurtrie, R.E. and Y.P. Wang. 1993. Mathematical models of the photosynthetic responses of tree stands to rising CO_2 concentrations and temperatures. Plant Cell Environ. 6:1–13.

Miron, D. and A.A. Schaffer. 1991. Sucrose phosphate synthase, sucrose synthase, and invertase activities in developing fruit of *Lycopersicon esculentum* Mill. and the sucrose accumulating *Lycopersicon hirsutum* Humb. and Bonpl. Plant Physiol. 95:623–627.

Mishra, D., S. Shekhar, L. Agrawal, S. Chakraborty, and N. Chakraborty. 2017. Cultivar-specific high temperature stress responses in bread wheat (*Triticum aestivum* L.) associated with physiochemical traits and defense pathways. Food Chem. 221:1077–1087.

Miyagi, M., H. Oku, and I. Chinen. 1990. Purification and action pattern on soluble starch of a-amylase from sugarcane leaves. Agr. Biol. Chem. 54:849–855.

Nakano, Y. and K. Asada. 1981. Hydrogen peroxide is scavenged by ascorbate specific peroxidase in spinach chloroplasts. Plant Cell Physiol. 22:679–690.

Patterson, B.D., E.A. Macrae, and I.B. Ferguson. 1984. Estimation of hydrogen peroxide in plants extracts using titanium (IV). Ann. Biochem. 139(2):487–492.

Sharma, D.K., S.B. Andersen, C.O. Ottosen, and E. Rosenqvist. 2014. Wheat cultivars selected for high Fv/Fm under heat stress maintain high photosynthesis, total chlorophyll, stomatal conductance, transpiration and dry matter. Physiol. Plant. 153:284–298.

Shu, S., L.Y. Yuan, S.R. Guo, J. Sun, and Y.H. Yuan. 2013. Effect of exogenous spermine on chlorophyll fluorescence, antioxidant system and ultrastructure of chloroplast in *Cucumis sativus* L. under salt stress. Plant Physiol. Biochem. 63:209–216.

Strain, H.H. and W.A. Svec. 1966. Extraction, separation, estimation and isolation of the chlorophylls, p. 21–66. In: L.P. Vernon and G.R. Seeley (eds.). The chlorophylls. Academic Press, New York.

Wahid, A. and E. Rasul. 2005. Photosynthesis in leaf stem, flower and fruit, p. 479–497. In: M. Pessarakli (ed.). Handbook of photosynthesis, 2nd edition. CRC Press, Boca Raton, Florida.

Wang, J.Z., L.J. Cui, Y. Wang, and J.L. Li. 2009. Growth, lipid peroxidation and photosynthesis in two tall fescue cultivars differing in heat tolerance. Biol. Plant. 53:237–242.

Xie, Z., L. Duan, X. Tian, B. Wang, E.A. Egrinya, and Z. Li. 2008. Coronatine alleviates salinity stress in cotton by improving the antioxidative defense system and radical-scavenging activity. J. Plant Physiol. 165:375–384.

Xu, P.L., Y.K. Guo, J.G. Bai, L. Shang, and X.J. Wang. 2008. Effects of long-term chilling on ultrastructure and antioxidant activity in leaves of two cucumber cultivars under low light. Physiol. Plant. 132:467–478.

Xu, S., J. Li, X. Zhang, H. Wei, and L. Cui. 2006. Effects of heat acclimation pretreatment on changes of membrane lipid peroxidation, antioxidant metabolites, and ultrastructure of chloroplasts in two cool-season turfgrass species under heat stress. Environ. Exp. Bot. 56: 274–285.

Yang, X., X. Chen, Q. Ge, B. Li, Y. Tong, A. Zhang, Z. Li, T. Kuang, and C. Lu. 2006. Tolerance of photosynthesis to photoinhibition, high temperature and drought stress in flag leaves of wheat: A comparison between a hybridization line and its parents grown under field conditions. Plant Sci. 171:389–397.

Yuan, L., S. Zhu, S. Li, S. Shu, J. Sun, and S. Guo. 2014. 24-Epibrassinolide regulates carbohydrate metabolism and increases polyamine content in cucumber exposed to $Ca(NO_3)_2$ stress. Acta Physiol. Plant. 36:2845–2852.

Zha, Q., X.J. Xi, A.L. Jiang, S.P. Wang, and Y.H. Tian. 2016. Changes in the protective mechanism of photosystem II and molecular regulation in response to high temperature stress in grapevines. Plant Physiol. Biochem. 101: 43–53.

Zhang, J., X.D. Jiang, T.L. Li, and X.J. Cao. 2014. Photosynthesis and ultrastructure of photosynthetic apparatus in tomato leaves under elevated temperature. Photosynthetica 52: 430–436.

Zheng, L., M. Su, X. Wu, and C. Liu. 2008. Antioxidant stress is promoted by nano-anatase in spinach chloroplasts under UV-B radiation. Biol. Trace Elem. Res. 121:69–79.

Zhou, R., X. Yu, K.H. Kjar, E. Rosenqvist, C. Ottosen, and Z. Wu. 2015. Screening and validation of tomato genotypes under heat stress using Fv/Fm to reveal the physiological mechanism of heat tolerance. Environ. Exp. Bot. 118:1–11.

Zou, M.Q., L.Y. Yuan, S.D. Zhu, S. Liu, J.T. Ge, and C.G. Wang. 2017. Effects of heat stress on photosynthetic characteristics and chloroplast ultrastructure of a heat-sensitive and a heat-tolerant cultivar of wucai (*Brassica campestris* L.). Acta Physiol. Plant. 39:30.